Fused-Ring Systems

Deutsche Ausgabe: DOI: 10.1002/ange.201503783
Internationale Ausgabe: DOI: 10.1002/anie.201503783

Electron-Deficient Tetrabenzo-Fused Pyracylene and Conversions into Curved and Planar π-Systems Having Distinct Emission Behaviors**

Chaolumen, Michihisa Murata, Yasunori Sugano, Atsushi Wakamiya, and Yasujiro Murata**

Abstract: *Polycyclic aromatic compounds containing fully unsaturated five-membered ring(s) have been intensively studied because of their unique properties, which include high electron affinity and reactivity. Reported herein is an efficient route for the synthesis of tetrabenzo-fused pyracylene, which comprises pyracylene and tetracene segments, using intramolecular oxidative C–H coupling. It was shown to possess high electron affinity and was found to undergo addition reactions with n-butyllithium or benzyne. These reactions led to either a 1,4-addition compound or triptycene-type adduct with a curved or planar π-system, respectively. Although these compounds exhibited similar sky-blue emissions in a dilute solution, the emission band of the 1,4-addition compound was significantly red-shifted in the solid state and exhibited intense yellow emission attributable to the excimer, while the triptycene-type adduct retained the intense blue color emission in the solid state.*

Polycyclic aromatic hydrocarbons (PAHs) containing fully unsaturated five-membered rings, so called cyclopenta-fused polycyclic aromatic hydrocarbons (CP-PAHs), have received attention because of their unusual properties such as high electron affinities[1] and chemical reactivities,[2] as well as for their potential use in organic electronic devices.[3] CP-PAH molecules such as rubicenes,[4] dithiarubicene (so called emeraldicenes),[5] and cyclopenta[*hi*]aceanthrylenes[6] have been reported as electron-accepting (n-type) and ambipolar materials for either organic photovoltaics (OPVs) or organic field-effect transistors (OFETs).

Among the CP-PAHs, pyracylene has been known to possess anti-aromatic character and high electron affinity, thus resulting from the contribution of 12π-electron periphery with a strongly localized interior double bond (1.35 Å).[7] In contrast, tetracene and derivatives thereof have attracted particular interest as excellent charge transporting materials.[8] In this work, we focused on the tetrabenzo-fused pyracylenes **1** (abbreviated as TBP), which includes both pyracylene and tetracene moieties, to elucidate its electronic properties and chemical reactivity (Scheme 1). Although the synthesis of **1** was reported in 1956 by Theiling et al.,[9] this method was recently reported to be low yielding.[10] Herein we report an efficient route for the synthesis of TBPs by intramolecular oxidative C–H coupling and its unique reactivity, thus leading to the formation of intriguing π-systems with distinct emission properties in the crystal form with high quantum yields. These addition reactions can provide ways to access highly fluorescent materials having unique three-dimensional structures.

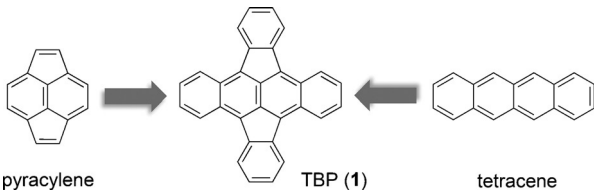

Scheme 1. Structures of TBP (**1**) and its key segments, pyracylene and tetracene.

The syntheses of the TBPs **1a–c** were conducted by Scholl reaction of the 5,11-diaryltetracene derivatives **3a–c** using $FeCl_3$ as an oxidant (Scheme 2). Monocyclization and double cyclization proceeded regioselectively at ambient conditions in a controlled manner, depending on the amount of $FeCl_3$, to

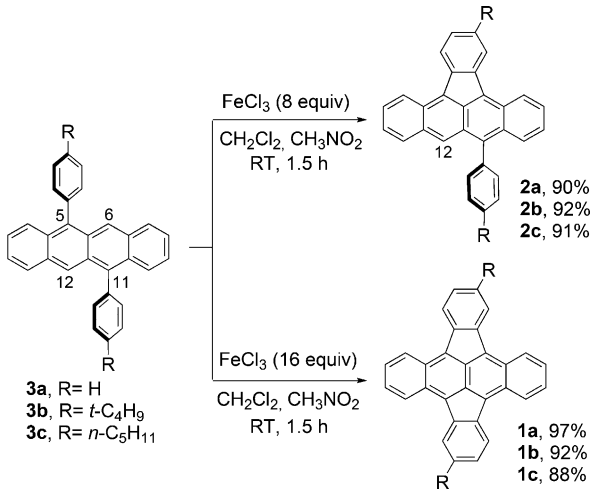

Scheme 2. Intramolecular oxidative cyclizations of the 5,11-diaryltetracene derivatives **3a–c**.

[*] Chaolumen, Dr. M. Murata, Y. Sugano, Prof. Dr. A. Wakamiya, Prof. Dr. Y. Murata
Institute for Chemical Research, Kyoto University
Uji, Kyoto 611-0011 (Japan)
E-mail: mmurata@scl.kyoto-u.ac.jp
yasujiro@scl.kyoto-u.ac.jp

[**] We are grateful to Prof. Jun Terao and Prof. Yasushi Tsuji for the quantum yield measurements. Financial support was provided by JSPS KAKENHI Grant Number 24350024. XRD measurements of the compound **1b** was carried out at SPring-8 (BL38B1) with the approval of JASRI (2012B1319 and 2013A1489). This study was carried out with the NMR spectrometer in the Joint Usage/Research Center (JURC) at ICR, Kyoto University.

Supporting information for this article is available on the WWW under http://dx.doi.org/10.1002/anie.201503783.

afford **2a–c** and **1a–c** as deep-purple and deep-blue solids, respectively. Whereas a similar reaction was recently reported for pentacene derivatives by Chi et al.,[11] the construction of a pyracylene moiety by the double cyclization is unprecedented. Although Scholl reactions are considered to proceed via either radical cation or arenium cation intermediates,[12] we confirmed that no cyclization of **3c** proceeded under acidic conditions with $MeSO_3H$, and is indicative of the radical cation mechanism. Actually, the DFT calculations (see the Supporting Information) for the radical cations $\mathbf{3a}^{\bullet+}$ and $\mathbf{2a}^{\bullet+}$ indicated that spin densities are relatively localized at C6 and C12 for $\mathbf{3a}^{\bullet+}$ and C12 for $\mathbf{2a}^{\bullet+}$. In addition, **1a** was calculated to be the most unstable in energy among the three possible isomers, thus suggesting that the cyclizations likely proceeded under kinetic control.

X-ray diffraction analyses were performed for **3a**, **2a**, and **1b** (Figure 1 a–c). The results show that the cyclizations of the two phenyl rings to form five-membered rings caused significant changes in the bond lengths. In particular, the bonds denoted as *a* were shortened [1.451(3) Å for **3a**, 1.417(2) Å for **2a**, 1.381(3) Å for **1b**], while the bonds *b* were elongated [1.442(2) Å for **3a**, 1.450(2) Å for **2a**, 1.474(2) Å for **1b**]. The enhanced double-bond character of bond *a* in **1b** appeared to be similar to the characteristics of pyracylene (the corresponding bond length is 1.35 Å).[13] In contrast, when we compare the structures of indeno moieties, bond *c* is elongated in **1b** [1.438(2) Å] after the second cyclization relative to bond *c* in **2a** [1.421(2) Å]. In addition there is a slight elongation of bonds *d* and *e* in **1b** [1.485(2) Å and 1.486(2) Å, respectively], compared to those bond lengths in **2a** [1.474(2) Å and 1.478(2) Å, respectively]. It is notable that bond *c* of **1b** is clearly longer than the corresponding bond in the parent pyracylene (1.366 Å),[13] and is likely a result of avoiding contributing to the anti-aromatic character. These data indicate that the major contribution to the resonance structure is form **A**, which is among the possible resonance structures, including form **B**, in which the 20π-antia-romatic periphery can be drawn (as shown with a bold line in Figure 1 d).

This consideration is supported by the results of DFT calculations.[14] The structural optimization for **1a–3a** calculated at the B3LYP/6-31G* level of theory reproduce the crystal structures well (see the Supporting Information). The NICS(0) (nucleus independent chemical shifts)[15] values for the optimized structures are summarized in Figure 2.

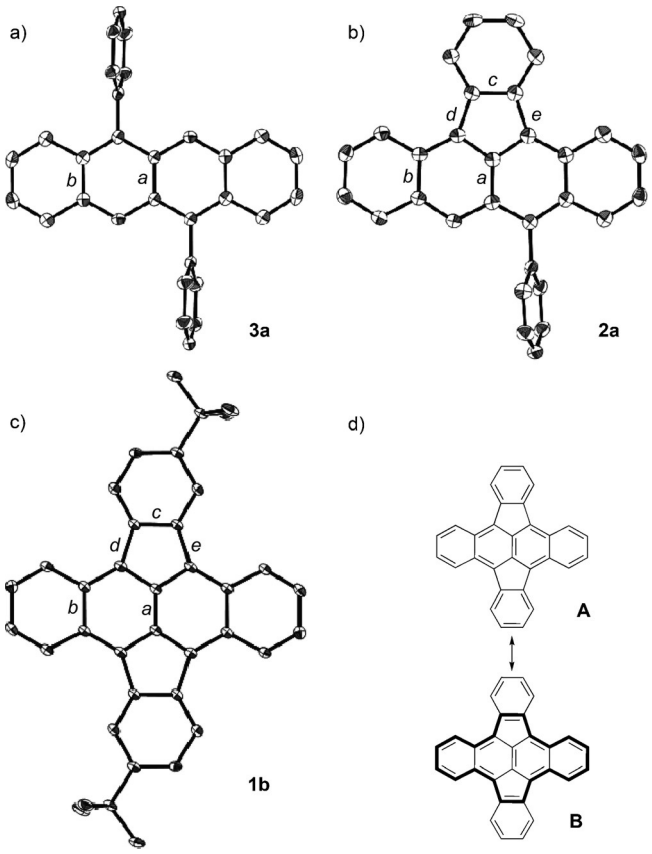

Figure 1. The ORTEP drawings (50% probability for thermal ellipsoids) of **3a** (a), **2a** (b), **1b** (c), and selected resonance structures of **1a** (d). Selected bond lengths [Å] for **3a**: bond *a* 1.451(3); *b* 1.442(2). Selected bond lengths [Å] for for **2a**: bond *a* 1.417(2); *b* 1.450(2); *c* 1.421(2); *d* 1.474(2); *e* 1.478(2). Selected bond lengths [Å] for **1b**: bond *a* 1.381(3); *b* 1.474(2); *c* 1.438(2); *d* 1.485(2); *e* 1.486(2).

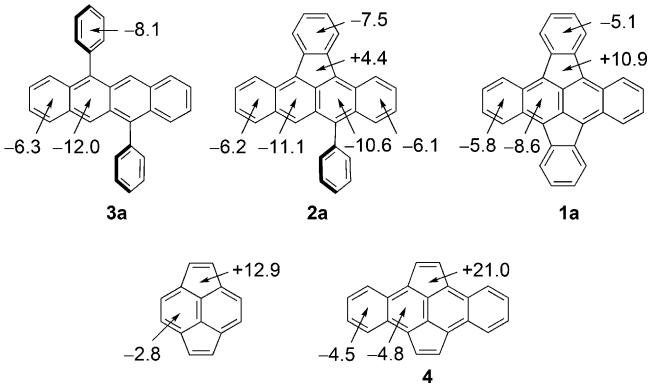

Figure 2. NICS(0) values for **1a–3a**, pyracylene, and dibenzo-fused pyracylene **4** calculated at the HF/6-311+G**//B3LYP/6-31G* level of theory.

Although the changes in the NICS(0) values after monocyclization are small, both the negative values for six-membered rings and the positive value for the five-membered ring become more positive in **1a**, with reference to **2a**, after the second cyclization. The NICS(0) calculations for the model compound **4** indicated that introduction of two fused rings on the naphthalene moiety in pyracylene significantly increases the positive values for five-membered ring compared to those for pyracylene (from +12.9 for pyracylene to +21.0 for **4**), and is indicative of the contribution of 20π-anti-aromatic periphery. The introduction of two fused rings on the two five-membered rings of **4** has a strong impact and weakens the anti-aromatic contribution, while enhancing the aromatic character in the tetracene moiety. Hence, we expected TBP to possess electronic properties analogous to both pyracylene and tetracene.

To clarify the electronic properties, we conducted cyclic voltammetry (CV) for **1b–3b**. In the reduction process, **3b** and **2b** exhibited one reversible reduction wave ($E_{1/2}$ =

−2.11 V vs. Fc/Fc^+ for **3b** and −1.64 V for **2b**). The formation of one indeno moiety causes a positive shift of the potential of **2b**, with reference to **3b**, by $\Delta E_{1/2} = 0.47$ V. The compound **1b** exhibited two reversible waves ($E_{1/2} = -1.30$ V and −1.76 V) with the first reduction potential shifted to a more positive value by $\Delta E_{1/2} = 0.34$ V compared to that of **2b**, and is indicative of high electron affinity of the TBP skeleton. In the oxidation process, **3b** and **2b** exhibited one reversible oxidation wave ($E_{1/2} = +0.43$ V for **1b** and +0.55 V for **2b**), but the difference ($\Delta E_{1/2} = 0.12$ V) is apparently smaller than those observed in the reduction process. The shape of the oxidation wave of **1b** ($E_{pa} = +0.49$ V) was broad but reproducible for several cycles, in a range of +1.0 to −2.0 V, and indicative of the effect of aggregation.

The absorption spectra were also measured and the data, together with that of CV, are summarized in Table 1.

Table 1: Optical and electrochemical data.

Compd.	Oxidation potential[a] $E_{1/2}$ [V]	Reduction potential[a] $E_{1/2}$ [V]	LUMO[b] (eV)	Absorption[c] λ_{max} [nm]	$\log\varepsilon$
3b	0.43	−2.11	−2.99	495	4.04
2b	0.55	−1.64	−3.46	579	3.93
1b	(0.49)	−1.30	−3.80	613	4.28

[a] In CH_2Cl_2 with $(n\text{Bu})_4N^+PF_6^-$ (0.1 M) as a supporting electrolyte at a scan rate of 100 $mV\,s^{-1}$ using ferrocene/ferrocenium as an internal standard. Peak oxidation potential (E_{pa}) in parenthesis. [b] LUMO energy level was calculated from the half wave potential of the first reduction wave by using the following equations: LUMO $= -(E_{1/2} + 5.1)$ (eV).[16] [c] In toluene.

Reflecting the low-lying LUMO, **1b** showed an intense absorption band ($\lambda_{max} = 613$ nm, $\log\varepsilon = 4.28$) which is notably red-shifted by 118 nm compared to that of **3b** ($\lambda_{max} = 495$ nm, $\log\varepsilon = 4.04$), and by 34 nm compared to that of **2b** ($\lambda_{max} = 579$ nm, $\log\varepsilon = 3.93$). Considering the electron affinity and the absorption profile, TBP can be used as a potential building block for n-type materials in OPVs.[1c,4d]

Unique addition reactions[17] or substitution reactions[5a] of CP-PAHs with alkyllithium reagents have been reported, so we also studied the reactivity of TBP. When *n*-butyllithium was added to a suspension of **1a** in THF at −78 °C, the dark-blue powder of **1a** smoothly dissolved to afford a deep-purple solution. Quenching this solution with *n*-butyliodide or acidic water provided the 1,4-addition products **6a**,**b** (Scheme 3). The compounds **6a**,**b** have a curved π-surface as confirmed by the single-crystal X-ray diffraction analyses (see below). The LUMO of **1a** delocalizes over the entire molecular surface except for the interior double bond (Figure 3a). We anticipated *n*-butyllithium to kinetically attack one of the carbon atoms in the five-membered rings, atoms for which orbital coefficients are relatively large, to give the cyclopentadienyl-type anion **5a**. The HOMO of anion **5a** is localized on the five-membered ring with the highest coefficient at C12 (Figure 3b). Thus, the quenching reactions selectively proceeded at C12 to give **6a**,**b** under kinetic control. In addition, benzyne was found to undergo addition to **1a** to afford **7** with

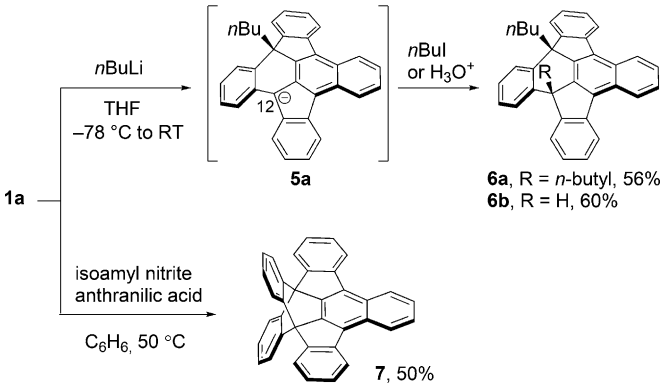

Scheme 3. Regioselective addition reactions of **1a**. THF = tetrahydrofuran.

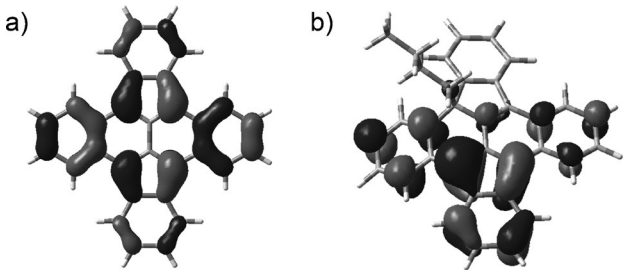

Figure 3. Plot of the LUMO of **1a** (a; B3LYP/6-31G*) and the HOMO of the anion intermediate **5a** (b; B3LYP/6-31 + G*).

an intriguing triptycene-type structure (Scheme 3), thus indicating that TBP retains the reactivity characteristics of tetracene.[18]

In a toluene solution, **6a** and **7** showed an absorption band in a similar region with the maximum wavelength (λ_{abs}) at 388 nm and 376 nm, respectively, which were hypsochromically shifted with reference to that of **1a** ($\lambda_{abs} = 611$ nm), thus reflecting the partial scission of the π-system of **1a** (Figure 4). The compounds **6a** and **7** (8.6×10^{-6} M and 7.1×10^{-6} M in toluene, respectively) exhibited intense sky-blue fluorescence with the maximum wavelength (λ_{em}) at 407 nm ($\Phi_F = 0.99$, $\tau = 3.2$ ns) and 383 nm ($\Phi_F = 0.98$, $\tau = 2.3$ ns), respectively. The rigidly fixed conformations of **6a** and **7** likely contribute to the small Stokes shifts (19 nm and 7 nm, respectively) as well as the high quantum yields. However, **6a** and **7** showed distinct emission behaviors in a concentrated solution and in the solid state, while the absorption profiles were almost unchanged. The compound **6a** exhibited a new red-shifted emission band ($\lambda_{em} = 509$ nm, $\Phi_F = 0.51$, $\tau = 7.1$ ns) in a higher concentration (7.9×10^{-3} M in toluene; Figure 4a).[19] The longer fluorescence lifetime for **6a** at a high concentration indicates that the red-shifted emission is attributable to the excimer.[20] Interestingly, the crystals of **6a** showed intense yellow emission at $\lambda_{em} = 547$ nm while keeping the high quantum yield ($\Phi_F = 0.88$). In contrast, the red-shift of the emission band for **7** was not remarkable and showed intense sky-blue emission in a concentrated solution ($\lambda_{em} = 404$ nm, $\Phi_F = 0.50$, $\tau = 2.8$ ns) as well as in the solid state ($\lambda_{em} = 441$ nm, $\Phi_F = 0.73$; Figure 4b).

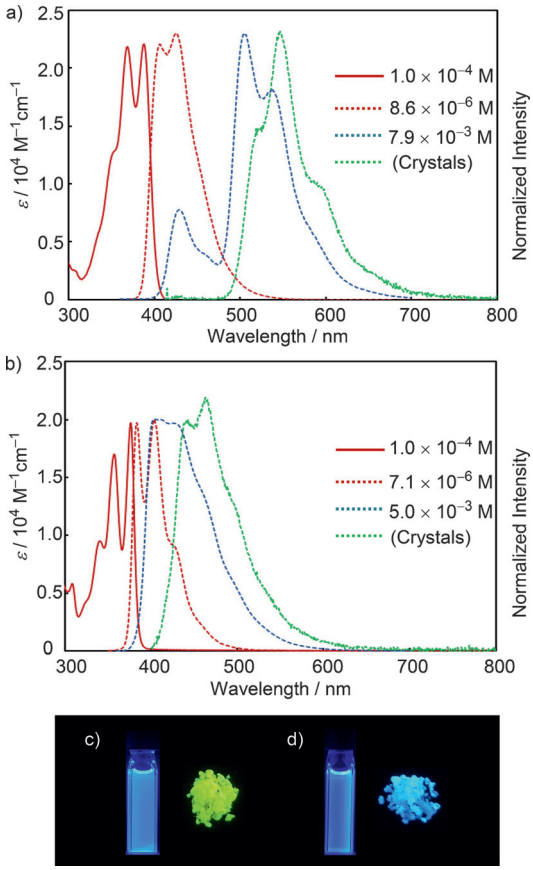

Figure 4. UV-vis absorption spectra (solid line) and normalized fluorescence spectra (dashed line) of **6a** (a) and **7** (b) in toluene and in the solid state. The pictures of the toluene solution and crystals of **6a** (c) and **7** (d) with irradiation at 365 nm (the concentrations of the solutions: 8.6×10^{-6} M and 7.1×10^{-6} M for **6a** and **7**, respectively).

The packing structures of **6a** and **7** in the solid state provided a better understanding of the difference in the emission behaviors. The compound **6a** has a curved π-system and forms a dimeric structure in a face-to-face fashion between the concave surfaces (Figure 5a). The distance between the mean planes of the overlapping naphthalene moieties (3.56 Å) is within a range that is typical of a π-stacked structure (3.4–3.7 Å). In contrast, the nearly-planar π-surface of **7** is arranged in a significantly slipped fashion (Figure 5b). Although the π-stacked distance of **7** measured between the mean plane of the naphthalene moiety and the closest carbon atom in the benzene moiety (3.45 Å) is shorter than that of **6a**, contacts between the π-systems in the dimer of **7** are small because of the slipped-stacking arrangement. From these data, we propose that the curved π-skeleton of **6a** restricts the geometry for the π–π interactions in such a way that the central naphthalene moieties can overlap effectively. This effect leads to the stabilization of the excimer of **6a** which shows markedly red-shifted emission in the solid state as compared to those of **7**.

In summary, we demonstrated an efficient route for the synthesis of electron-deficient tetrabenzo-fused pyracylene (TBP) and its derivatives by using intramolecular oxidative C–H coupling. The X-ray diffraction analysis showed that

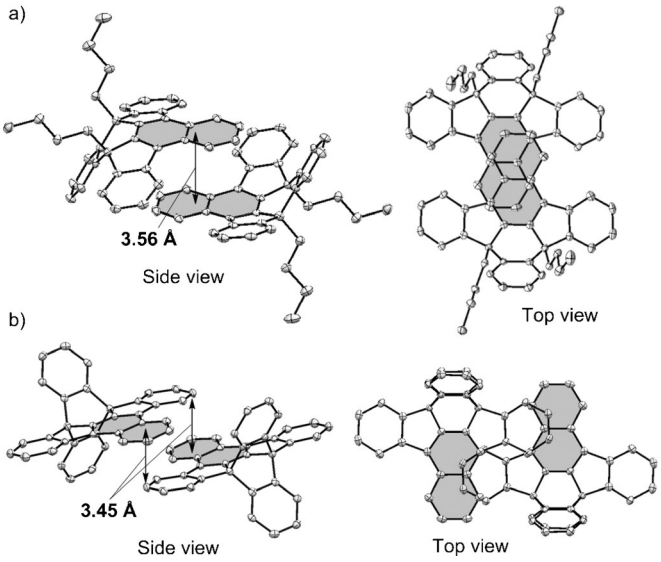

Figure 5. The face-to-face dimeric structures in the crystal of **6a** (a) and **7** (b).

TBP possesses structural features similar to both tetracene and pyracylene. We also disclosed that TBP undergoes unique addition reactions with *n*-butyllithium or benzyne to give either a 1,4-addition compound or triptycene-type adduct with a curved or planar π-surface, respectively. These compounds showed distinct emissions in the concentrated solution and solid state with high quantum yields. X-ray diffraction analyses demonstrated that the 1,4-addition compound forms dimers with effective π-overlap, which can cause a significant red-shift in the fluorescence by the stabilization of excimer. Further studies on larger CP-PAHs containing pyracylene segment(s) and their modifications are currently underway in our group.

Keywords: fluorescence · fused-ring systems · hydrocarbons · π interactions · X-ray diffraction

How to cite: *Angew. Chem. Int. Ed.* **2015**, *54*, 9308–9312
Angew. Chem. **2015**, *127*, 9440–9444

[1] a) F. G. Brunetti, X. Gong, M. Tong, A. J. Heeger, F. Wudl, *Angew. Chem. Int. Ed.* **2010**, *49*, 532–536; *Angew. Chem.* **2010**, *122*, 542–546; b) D. T. Chase, A. G. Fix, B. D. Rose, C. D. Weber, S. Nobusue, C. E. Stockwell, L. N. Zakharov, M. C. Lonergan, M. M. Haley, *Angew. Chem. Int. Ed.* **2011**, *50*, 11103–11106; *Angew. Chem.* **2011**, *123*, 11299–11302; c) J. D. Wood, J. L. Jellison, A. D. Finke, L. Wang, K. N. Plunkett, *J. Am. Chem. Soc.* **2012**, *134*, 15783–15789; d) H. Xia, D. Liu, X. Xu, Q. Miao, *Chem. Commun.* **2013**, *49*, 4301–4303.
[2] K. N. Plunkett, *Synlett* **2013**, 898–902.
[3] a) J. Nishida, S. Tsukaguchi, Y. Yamashita, *Chem. Eur. J.* **2012**, *18*, 8964–8970; b) D. T. Chase, A. G. Fix, S. J. Kang, B. D. Rose, C. D. Weber, Y. Zhong, L. N. Zakharov, M. C. Lonergan, C. Nuckolls, M. M. Haley, *J. Am. Chem. Soc.* **2012**, *134*, 10349–10352.
[4] a) M. Smet, J. V. Dijk, W. Dehaen, *Synlett* **1999**, 495–497; b) H. A. Wegner, L. T. Scott, A. de Meijere, *J. Org. Chem.* **2003**, *68*, 883–887; c) H.-H. Hseuh, M.-Y. Hsu, T.-L. Wu, R.-S. Liu, *J.*

Org. Chem. **2009**, *74*, 8448 – 8451; d) H.-Y. Chen, J. Golder, S.-C. Yeh, C.-W. Lin, C.-T. Chen, *RSC Adv.* **2015**, *5*, 3381 – 3385.
[5] a) A. R. Mohebbi, F. Wudl, *Chem. Eur. J.* **2011**, *17*, 2642 – 2646; b) A. R. Mohebbi, J. Yuen, J. Fan, C. Munoz, M. Wang, R. S. Shirazi, J. Seifter, F. Wudl, *Adv. Mater.* **2011**, *23*, 4644 – 4648.
[6] a) H. Dang, M. A. Garcia-Garibay, *J. Am. Chem. Soc.* **2001**, *123*, 355 – 356; b) H. Dang, M. Levitus, M. A. Garcia-Garibay, *J. Am. Chem. Soc.* **2002**, *124*, 136 – 143; c) C. L. Eversloh, Y. Avlasevich, C. Li, K. Müllen, *Chem. Eur. J.* **2011**, *17*, 12756 – 12762.
[7] H. P. Diogo, T. Kiyobayashi, M. E. Minas da Piedade, N. Burlak, D. W. Rogers, D. McMasters, G. Persy, J. Wirz, J. F. Liebman, *J. Am. Chem. Soc.* **2002**, *124*, 2065 – 2072.
[8] a) J. E. Anthony, *Chem. Rev.* **2006**, *106*, 5028 – 5048; b) J. E. Anthony, *Angew. Chem. Int. Ed.* **2008**, *47*, 452 – 483; *Angew. Chem.* **2008**, *120*, 460 – 492; c) M. Mas-Torrent, C. Rovira, *Chem. Rev.* **2011**, *111*, 4833 – 4856.
[9] a) K. F. Lang, E.-A. Theiling, *Chem. Ber.* **1956**, *89*, 2734 – 2737; b) A. Bennett, A. W. Hanson, *Acta Crystallogr.* **1953**, *6*, 736 – 739.
[10] X. Gu, W. A. Luhman, E. Yagodkin, R. J. Holmes, C. J. Douglas, *Org. Lett.* **2012**, *14*, 1390 – 1393.
[11] A. Naibi Lakshminarayana, J. Chang, J. Luo, B. Zheng, K.-W. Huang, C. Chi, *Chem. Commun.* **2015**, *51*, 3604 – 3607.
[12] L. Zhai, R. Shukla, S. H. Wadumethrige, R. Rathore, *J. Org. Chem.* **2010**, *75*, 4748 – 4760.
[13] B. Freiermuth, S. Gerber, A. Riesen, J. Wirz, M. Zehnder, *J. Am. Chem. Soc.* **1990**, *112*, 738 – 744.
[14] Gaussian 09 (Revision C.01), M. J. Frisch, et al. Gaussian, Inc., Wallingford CT, **2010**. For full references, see the Supporting Information.
[15] P. v. R. Schleyer, C. Maerker, A. Dransfeld, H. Jiao, N. J. R. v. E. Hommes, *J. Am. Chem. Soc.* **1996**, *118*, 6317 – 6318.
[16] C. M. Cardona, W. Li, A. E. Kaifer, D. Stockdale, G. C. Bazan, *Adv. Mater.* **2011**, *23*, 2367 – 2371.
[17] a) H. E. Bronstein, L. T. Scott, *J. Org. Chem.* **2008**, *73*, 88 – 93; b) A. Hirsch, M. Brettreich, *Fullerenes-Chemistry and Reactions*, Wiley-VCH, Weinheim, **2005**.
[18] M. Sugihashi, R. Kawagita, T. Otsubo, Y. Sakata, S. Misumi, *Bull. Chem. Soc. Jpn.* **1972**, *45*, 2836 – 2841.
[19] C. E. Kalmus, D. M. Hercules, *J. Am. Chem. Soc.* **1974**, *96*, 449 – 456.
[20] a) K. Nagura, S. Saito, H. Yusa, H. Yamawaki, H. Fujihisa, H. Sato, Y. Shimoikeda, S. Yamaguchi, *J. Am. Chem. Soc.* **2013**, *135*, 10322 – 10325; b) P. Galer, R. C. Korošec, M. Vidmar, B. Šket, *J. Am. Chem. Soc.* **2014**, *136*, 7383 – 7394.

Received: April 25, 2015
Published online: June 18, 2015

